Boronate-ester crosslinked hyaluronic acid hydrogels for dihydrocaffeic acid delivery and fibroblasts protection against UVB irradiation

Mariana Maciel de Oliveira, Celso Vataru Nakamura, Rachel Auzély-Velty

Boronate-ester crosslinked hyaluronic acid hydrogels for dihydrocaffeic acid delivery and fibroblasts protection against UVB irradiation

Mariana Maciel de Oliveira[a], Celso Vataru Nakamura[a], Rachel Auzély-Velty[b,*]

[a] Universidade Estadual de Maringá, Maringá, 87020900, Brazil

[b] University Grenoble Alpes, Centre de Recherches sur les Macromolécules Végétales (CERMAV)-CNRS, Grenoble, 38041, France

[*]Corresponding author.

Tel.: +33 04 76 03 76 71

E-mail address: rachel.auzely@cermav.cnrs.fr (R. Auzély-Velty).

Univ Grenoble Alpes, CERMAV-CNRS, Grenoble, 38041, France

Abstract

Herein, we exploit the dynamic nature and pH dependence of complexes between phenylboronic acid and diol-containing molecules to control the release of an anti-photoaging agent, dihydrocaffeic acid (DHCA), from a dynamic covalent hydrogel (HG). The HG is prepared by reversible formation of boronate ester crosslinks between hyaluronic acid (HA) modified with saccharide (GLU) residues and HA functionalized with 3-aminophenylboronic acid (APBA), part of which is involved in complexation with DHCA. The hydrogel exhibited increased dynamic moduli and a lower relaxation time at pH 7.4 in comparison to pH 6, and greater amount of DHCA was incorporated at pH 7.4. Moreover, this hydrogel prolonged DHCA release at pH 7.4 through drug

reversible complexation/decomplexation, while the rate of release was fastest in acidic (skin) conditions. Very interestingly, the incorporation of DHCA into the network enhances its protection against UVB-induced L929 fibroblast death. Therefore, this smart hydrogel can contribute to photoaging prevention.

Keywords: hyaluronic acid, dynamic covalent hydrogel, dihydrocaffeic acid, anti-photoaging, small molecules delivery

1. Introduction

Human skin is the largest organ and the major protective barrier of the body. Consequently, it is continuously exposed to external harmful insults, especially ultraviolet radiation (UV) (Cavinato & Jansen-Dürr, 2017). UVB (280-320 nm) passes through epidermis and reaches the upper layer of dermis (Britto, Shanthakumari, Agilan, Radhiga, & Kanimozhi, 2017). Exposure to UVB causes oxidative stress by simultaneously increasing reactive oxygen species (ROS) production and decreasing endogenous antioxidants. Oxidative stress induced by UVB promotes a set of alterations in skin cells, which leads to photoaging, and is a key risk factor to skin cancer development (Cavinato & Jansen-Dürr, 2017; Dunaway, Odin, Zhou, Ji, & Zhang, 2018).

Several natural antiaging products have emerged, which can counteract UVB-induced skin damages by modulating some deleterious processes, including oxidative stress and inflammation (Cavinato, Waltenberger, Baraldo, Grade, & Jansen-Durr, 2017). The active compounds have been incorporated in various delivery systems in order to improve their efficiency of release in the skin as well as their photochemoprotective capacity. Micro/nanoemulsions, polymeric nanoparticles and

other nanocarriers have been extensively studied (Bagde, Mondal, & Singh, 2018). However, there are some limitations to using these systems, among them batch-to-batch variation, shelf stability and cost of production. In addition, the effectiveness of some formulations has not been studied yet (Bagde et al., 2018; Cavinato et al., 2017). Thus, there is a need for alternative approaches for the prevention of detrimental effects of UVB in skin.

In this context, hydrogels are interesting candidates as platforms for antiaging agent delivery. Indeed, as hydrophilic polymer networks (Nie, Pei, Wang, & Hu, 2018), hydrogels have drawn special attention for pharmaceutical and biomedical applications due to their high moisture content, soft and flexible structure, transparency, biocompatibility, biodegradability, non-toxicity and capacity to modify or control drug release (Kostova et al., 2018; Sahiner et al., 2015; Trombino et al., 2009). Several natural and synthetic polymers can be used to prepare hydrogels. Hyaluronic acid (HA) is a natural polymer composed of a repeating disaccharide unit of D-glucuronic acid and *N*-acetyl-D-glucosamine, linked by β-1,4 and β-1,3 glycosidic bonds (Essendoubi et al., 2016). HA presents beneficial properties for the skin, such as hydration, skin repair and wound healing, as well as unique physico-chemical properties, including viscoelasticity, high water retention capacity and lubrication. Moreover, HA can be chemically modified to obtain systems responsive to external stimuli. Hence, HA is widely used in the pharmaceutical and cosmetic fields as an active ingredient and to develop different topical drug delivery systems (Avadhani et al., 2017; Este, Eglin, & Alini, 2014; Sahiner et al., 2015). As HA cannot form a hydrogel itself, reversible crosslinking via dynamic covalent bonds has emerged as an attractive strategy to obtain HA-based networks (Figueiredo et al., 2019; Lou et al., 2018; Nimmo, Owen, & Shoichet, 2011). Among dynamic covalent bonds, boric acid and boronic acid

derivatives have been widely used to crosslink diol-containing polymers like polysaccharides as they can readily form reversible borate and boronate esters with 1,2- and 1,3-diol-containing species (Figueiredo, Ogawa, et al., 2020; Mayumi, Marcellan, Ducouret, Creton, & Narita, 2013; Sacco, Furlani, Paoletti, & Donati, 2019). In particular, crosslinking via phenylboronic acid (PBA or its derivatives) has been largely reported as it can be easily grafted on a polymer and can react with saccharides (or catechols) to form boronate esters that undergo hydrolysis under acidic conditions (Huang et al., 2018). Therefore, dynamic covalent crosslinks formed between PBA and saccharide molecules grafted on HA chains can be advantageously used to produce pH-responsive hydrogels (Figueiredo, Cosenza, et al., 2020; Heleg-Shabtai, Aizen, Orbach, Aleman-Garcia, & Willner, 2015; Roberts, Hanson, Massey, Karren, & Kiser, 2007; Tarus et al., 2014; Xu et al., 2011).

This is particularly interesting for epidermal application, since normal human skin exhibits an acidic pH (ranging from 3.0 to 6.5) (Duffy, Guzman, Wallace, Murphy, & Morrin, 2017). Dynamic covalent hydrogels offer many other advantages, including rapid and ease of preparation, flexibility to alter their structure like physically crosslinked networks while being more stable (Brooks & Sumerlin, 2016; Marco-Dufort & Tibbitt, 2019; Xu et al., 2011). Therefore, all these properties make such hydrogel networks attractive candidates for topical application. Accordingly, the purpose of the present study was to incorporate an antioxidant compound, dihydrocaffeic acid (DHCA), in a dynamic covalent hydrogel based on HA modified with PBA and saccharide moieties (Fig. 1), and to evaluate the potential of this smart polysaccharide network to control DHCA release and enhance cytoprotection produced against UVB death on fibroblasts.

Dihydrocaffeic acid (DHCA) is a phenolic compound with high antioxidant potential described in the literature (Amić, Marković, Klein, Dimitrić Marković, & Milenković, 2018; Poquet, Clifford, & Williamson, 2008), and it demonstrated cytoprotective effect on keratinocytes irradiated with UV (Poquet et al., 2008). Moreover, our previous studies showed that DHCA decreased some cellular oxidative harms, matrix metalloproteinases (MMPs) expression and apoptosis by decreasing ROS production, enhancing endogenous antioxidant defense and inhibiting mitogen-activated protein kinase (MAPK) pathway on L929 fibroblasts irradiated with UVB (Oliveira et al., 2019). Therefore, the development of a topical delivery system containing DHCA is an interesting strategy to prevent photoaging. Interestingly, once included in the HA-based dynamic covalent hydrogel described above, DHCA may form dynamic covalent bonds with PBA groups. This is the case as DHCA contains a catechol in its chemical structure. Thus, the selective entrapment of DHCA through complexation with PBA could be an attractive alternative to obtain an antiaging product with a controlled topical release of the active ingredient.

Some work have used hydrogels based on HA-catechol to obtain interesting skin care systems, as reported by Liang and colleagues (Liang et al., 2019). In this study, the authors developed adhesive hemostatic conductive hydrogels based on HA modified with dopamine and polydopamine-coated reduced graphene oxide using hydrogen peroxide/horseradish peroxidase as initiator system. The hydrogels demonstrated a set of interesting properties, especially for the skin, such as tissue adhesiveness, self-healing ability, wound healing, antioxidant capacity conferred by the catechol dopamine, and prolonged drug release.

Finally, although other studies have shown the interest of boronate ester-crosslinked hydrogels for control anticancer drug delivery (Heleg-Shabtai et al., 2015;

Huang et al., 2018), the reported process of drug release was based on the hydrogel dissociation. This was the case as the active species acted as cross-linkers in the polymer network. Conversely, in our case, the anti-photoaging agent DHCA does not cross-link the polymer chains. Consequently, the HA network can be obtained without the presence of DHCA, and its release from the hydrogel is not expected to promote its dissociation.

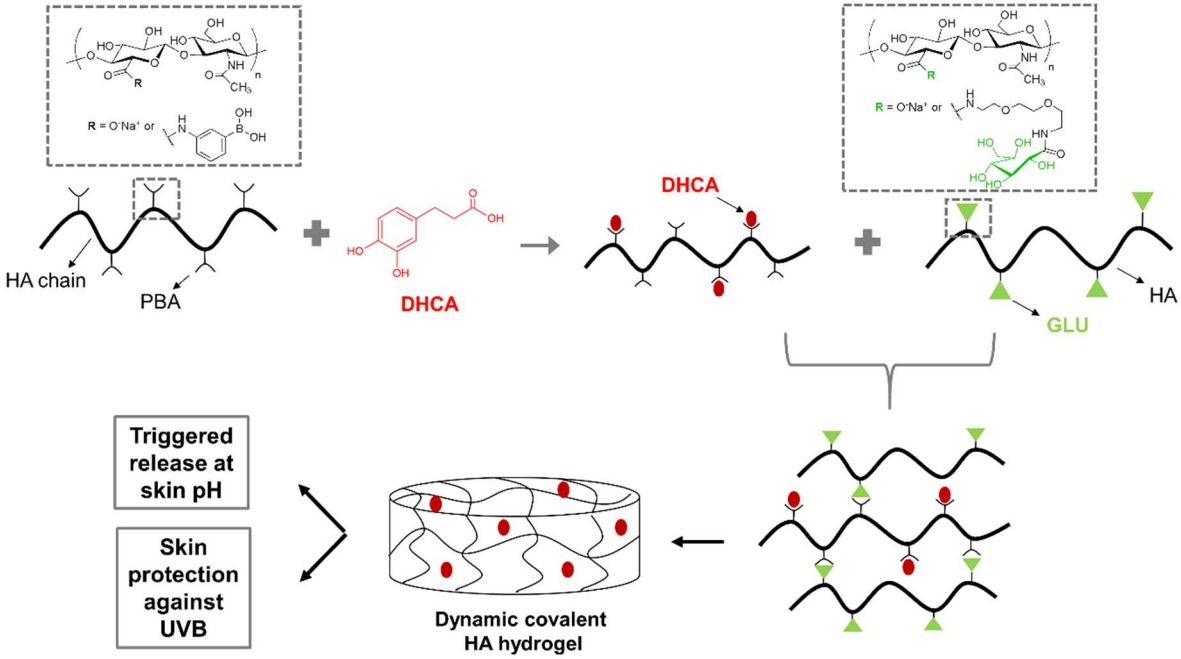

Figure 1: DHCA complexation by HA-PBA and production of HG containing DHCA via reversible boronate ester bond formation.

2. Experimental section

2.1. Materials

Sodium hyaluronic acid (HA, weight-average molar mass (M_w): 100 kg/mol) was obtained from Lifecore Biomedical. DHCA, 3-aminophenyl boronic acid (APBA), Hank's balanced salt solution (HBSS), *N*-acetyl cysteine (NAC), phosphate buffer saline (PBS) and 2,4,6-trinitrobenzene sulfonic acid (TNBS) were purchased from

Sigma-Aldrich. 4-(4,6-dimethoxy-1,3,5-triazin-2-yl)-4-methylmorpholinium chloride (DMTMM) and D-glucono-1,5-lactone were provided by Alfa Aesar and Carbosynth, respectively. Boc-1-amino-3,6-dioxa-8-octanamine (Boc-DOOA) was purchased from Iris Biotech GMBH. Dulbecco's modified Eagle's medium (DMEM) and fetal bovine serum (FBS) were purchased from Life Technologies/Gibco Laboratories. Neutral red was obtained from Interlab. All other solvents and chemicals used were of analytical grade. Water used in all the experiments was purified by using an Elga Purelab purification system, with a resistivity of 18.2 MΩ cm.

2.2. Determination of the binding affinity (K_a) of DHCA for APBA

In order to evaluate the affinity of DHCA for APBA, we determined the K_a by ^{1}H NMR spectroscopy (Bérubé, Dowlut, & Hall, 2008). In this assay, a 1:1 binding stoichiometry was assumed. The samples were diluted in deuterated PBS 0.01 M pD 6 or pD 7.4, and six different mixtures with a molar ratio of APBA/DHCA ranging from 1 to 2 were obtained (detailed procedure in supplementary material, Fig. S1 and S2). ^{1}H NMR spectra of APBA alone and of APBA in the presence of excess DHCA (to induce 100% complex formation) were recorded to assign the aromatic proton signals of bound and unbound APBA. The K_a was calculated by integration of aryl protons of the APBA/DHCA complex and of free APBA (equations described in supplementary material). The ^{1}H NMR spectra were recorded on a Bruker spectrometer operating at 400 MHz (Avance III HD model, Bruker BioSpin AG, Fallanden, Switzerland), at room temperature. Chemical shifts were given relative to external tetramethylsilane (TMS = 0 ppm) and calibration was performed using the signal of the residual protons of the solvent as a secondary reference.

2.3. Synthesis of HA-derivatives

HA grafted with APBA moieties (HA-PBA) was synthesized by an amide coupling reaction using APBA, HA and DMTMM as a coupling agent. APBA (93 mg, 0.50 mmol) was added to a water/dimethylformamide (water/DMF, 3:2 v/v) mixture containing DMTMM (212 mg, 0.77 mmol) and HA (306.6 mg, 0.77 mmol), and the pH was adjusted to 6.5 using 1 M aqueous solution of NaOH. The mixture was stirred for 46 h at room temperature. The resulting HA-PBA was purified by extensive dialysis against water (Spectra/Pore, MWCO 6-8 kD) followed by freeze drying (yield: 50%). The degree of substitution (DS, average number of substituting groups per repeating disaccharide unit of HA) of the final product was found to be 0.5 from ^{1}H NMR analyses (Tarus et al., 2014) using digital integration of the signals at δ (ppm) 6.8-7.9 (protons of APBA) and 2.0 (methyl protons in HA). This value was confirmed by that derived from the reaction kinetics using the TNBS method (supplementary material, Fig. S3).

HA grafted with gluconamide moieties (HA-GLU) was obtained in three steps (Figueiredo, Cosenza, et al., 2020). Firstly, a solution of D-glucono-1,5-lactone (80.8 mg, 0.45 mmol) in DMF (20 mL) was dropped in a solution of boc-DOOA (113 mg, 0.45 mmol) in DMF (25 mL) for 3 h. After stirring overnight at room temperature, the solvent was removed under reduced pressure, and the resulting product was dried under vacuum to give boc-DOOA-gluconamide (Fig. S4). In a second step, the boc protecting group was removed by acid treatment of boc-DOOA-gluconamide (56 mg, 0.13 mmol) in trifluoroacetic acid (0.6 mL, 7.8 mmol) for 5 min at room temperature. The pH of the mixture was adjusted to 7.0, and the solvent was removed under reduced pressure, yielding 1-amino-DOOA-gluconamide (Fig. S5). Then, the HA-GLU was synthesized by an amide coupling reaction. 1-amino-DOOA-gluconamide (56 mg, 0.17 mmol) was added to a water/DMF (3:2 v/v) mixture containing DMTMM (207 mg, 0.75 mmol) and

193 HA (300 mg, 0.75 mmol), and the pH was adjusted to 6.5 using 1 M aqueous solution
194 of NaOH. The mixture was stirred for 65 h at room temperature. The HA-GLU obtained
195 was purified by dialysis against water (Spectra/Pore, MWCO 6-8 kD) followed by
196 freeze-drying (yield: 84%). The DS of the HA-GLU conjugate was found to be 0.1 from
197 the reaction kinetics using the TNBS method (supplementary material, Fig. S3), and
198 was confirmed by ^{13}C NMR analyses (Fig. S6).
199
200 **2.4. HPLC analysis of DHCA**
201 Prominence High Performance Liquid Chromatography (HPLC) system
202 (Shimadzu, Kyoto, Japan), containing vacuum degasser, double micro-volume piston
203 pump, auto-sampler, thermostatic column compartment and spectrophotometer
204 detector UV-Vis and LabSolutions Software was used to analyze DHCA. Reversed-
205 phase chromatography was performed on a C_{18} column (150 × 3.0 mm, particle size 5
206 µm; Shimadzu, Kyoto, Japan). The mobile phase used was 0.01% (v/v) acetic acid in
207 water and acetonitrile (85:15 v/v), pH 3.8. The injection volume was 15 µL, with a flow
208 rate of 1 mL/min and column temperature of 25 °C. Elution was monitored for 6 min by
209 absorbance at 225 nm.
210 The validation of the proposed reversed-phase HPLC procedure was performed
211 according to International Conference on Harmonization of Technical Requirements
212 for Registration of Pharmaceuticals for Human Use Q2(R1) (ICH, 2005). The retention
213 time of DHCA was 2.4 min. The method was specific (Fig. S7) and linear (y = 24319x
214 + 4852.1, r = 0.9998) using eight concentrations in the range of 0.1–100 µg/mL of
215 DHCA. The residue analysis showed that the method presented significant regression
216 because the calculated F for regression was higher than critical F (110286.7 > 4.04),
217 and did not present lack of fit, regarding the calculated F for lack of fit was lower than

218 critical F (2.33 < 2.39). Moreover, the method presented accuracy and precision (Table
219 1S). Slight changes in mobile phase constitution (84:16 v/v) and column temperature
220 (24 °C) did not alter the DHCA quantification (Table S1), indicating that the method is
221 robust. The limit of detection and quantification were found to be 0.40 µg/mL and 1.22
222 µg/mL, respectively.
223
224 **2.5. Complexation of DHCA by HA-PBA**
225 DHCA was complexed with HA-PBA using a DHCA/PBA molar ratio of 1 in 0.01
226 M PBS pH 6 or pH 7.4 by stirring at 400 rpm for 30 min at room temperature. Non-
227 complexed DHCA was removed by centrifugation (7000 rpm, 15 min) using centrifugal
228 filter devices (Amicon Ultra - 15 mL centrifugal filter unit with Ultracel - 50 K membrane,
229 NMWL 50 kDa, Millipore, Cork, Ireland). After centrifugation, 50 µL of DHCA
230 complexed with HA-PBA (HA-PBA-DHCA), which was retained on the filter, were
231 diluted in acetonitrile in a ratio of 1:4 (sample:acetonitrile, v/v) and stirred for extraction
232 of DHCA. An aliquot of the resulted solution was diluted in water in a ratio of 1:5
233 (sample:water, v/v), filtered in micro filter (0.45 µM) and analyzed by HPLC. The DHCA
234 complexation efficiency (DCE) was calculated according to equation 1:
235 DCE (%) = (weight of complexed DHCA/initial weight of DHCA in the system)×100% (1)
236
237 **2.6. Formation of dynamic covalent HA hydrogels (HG)**
238 The HG were obtained by mixing different volumes of HA-PBA/DHCA complex
239 and HA-GLU solutions (15 g/L) in 0.01 M PBS pH 6 or pH 7.4, with a PBA/GLU molar
240 ratio of 1 (Tarus et al., 2014) (Fig. S8). Plain HG were obtained by mixing HA-PBA and
241 HA-GLU solutions with the same PBA/GLU molar ratio as described above for HG
242 containing DHCA (Fig. S9).

2.7. Oscillatory rheometry

The oscillatory rheological analyses of freshly prepared plain HG and HG containing DHCA produced at pH 6 or pH 7.4 were carried out at 32 °C, using a cone-plate AR2000 rheometer (TA Instruments, New Castle, USA) with a film of solvent trap (silicone) to avoid solvent evaporation. The cone used is striated, has a diameter of 20 mm, an angle of 4° and was separated by a fixed distance of 0.118 mm. Oscillatory strain sweep experiments at 1 Hz were used to determine the linear-viscoelastic range of the hydrogel networks as shown in Fig. S10. The oscillatory frequency sweep (0.01-10 Hz) experiments were performed within the linear viscoelastic range (strain fixed at 1.5 %) to determine the frequency dependence of the storage (G') and loss (G") moduli. The frequency dependences of the G' and G'' moduli were measured from at least three replicate samples.

2.8. *In vitro* DHCA release from HG

DHCA release from HG produced at pH 7.4 was performed in a Falcon cell culture insert (Corning Life Sciences, Durham, USA), containing a poly(ethylene terephthalate) track-etched membrane (0.4 µM pore size), mounted in a 24 well plate (Fig. S11). HG containing DHCA (300 mg), or 300 µL of DHCA dispersed in purified water was placed in the donor compartment, and kept in contact with 1 mL of receptor medium (0.01 M PBS pH 6 or pH 7.4). The system was maintained under stirring (450 rpm) at 32 ºC, and an aliquot of 500 µL was withdrawn at 0.5, 1, 2, 4, 6 and 8 h, and replaced with the same volume of receptor medium. The amount of DHCA released over time was determined by HPLC using the methodology previously validated. All experiments were carried out in triplicate.

2.9. Cell viability assay

Fibroblast L929 cell line (NCTC clone 929 [L cell, L929, derivative of Strain L] ATCC® CCL1™) was maintained and cultured in DMEM supplemented with 2 mM L-glutamine, 10% (v/v) FBS, penicillin (50 U/mL), and streptomycin (50 μg/mL) at 37 °C in a 5% CO_2 atmosphere.

Neutral red assay (Borenfreund & Puerner, 1985) was used to evaluate the cytotoxicity of DHCA, plain HG and HG containing DHCA produced at pH 7.4 on L929 cells. The cultured cell suspension was dispensed into a 96-well plate (2.5×10^4 cells/well) and incubated for 24 h. Thereafter, the media was replaced with serum-free DMEM containing different concentrations of DHCA (7, 14, 21, 28 and 35 μM), of HG without and with DHCA (amount of hydrogels containing 7, 14, 21, 28, and 35 μM of DHCA), and incubated for 24 h. PBS was used to wash the monolayers after incubation, and 200 μL of neutral red solution (40 μg/mL) was added. After 3 h the supernatant was removed and the cells were fixed with an aqueous solution of 2% (v/v) formaldehyde and 1% (w/v) calcium chloride, and then 200 μL of a solution of 1% (v/v) acetic acid and 50% (v/v) ethanol was added. Absorbance was measured at 540 nm (BioTek, PowerWave XS microplate spectrophotometer) after 15 min at 25 °C in the dark. The percentage of viable cells was calculated relative to untreated cells. The cytotoxicity analyses were determined in triplicate.

2.10. Cytoprotection assay against UVB

Neutral red assay was also used to evaluate the capacity of samples to protect L929 cells against UVB-induced death. L929 cells were seeded into 24-well plates (1.25×10^5 cells/well) and incubated for 24 h. After incubation, L929 cells were pre-

293 treated for 1 h with DHCA (7, 14, 21, 28, and 35 μM), HG without and with DHCA
294 produced at pH 7.4 (containing 7, 14, 21, 28, and 35 μM of DHCA) or 1 mM NAC (as
295 a positive control) dissolved in serum-free DMEM. Then, the media with treatments
296 was replaced by HBSS, and cells were irradiated with 600 mJ/cm^2 of UVB, a dose that
297 causes 50% cell death [OLIVEIRA et al., 2018]. One UVB lamp (Philips, TL 40W/12
298 RS SLV) at a fixed distance of 20 cm from the surface of the cell culture plates was
299 used. The irradiation intensity was measured by radiometer (Vilber Lourmat, VLX-3W,)
300 equipped with a sensor to detect UVB (detects peak of 312 nm) (Vilber Lourmat, CX-
301 312). After irradiation, cells were incubated for 24 h in serum-free DMEM, and then
302 were submitted to neutral red assay (Borenfreund & Puerner, 1985). The percentage
303 of viable cells was calculated relative to untreated and nonirradiated cells. The
304 analyses were carried out in triplicate.
305
306 ### 2.11. Statistical analysis
307 Data were expressed as the mean ± standard deviation (SD). Statistical analysis
308 was carried out by Prisma 5.0 software using one-way analysis of variance (ANOVA)
309 followed by Tukey test. Values of $p < 0.05$ were considered statistically significant.
310
311
312 ## 3. Results and Discussion
313
314 ### 3.1. Affinity of DHCA for APBA
315 To verify the ability to selectively entrap DHCA in the HA hydrogel through
316 complexation with APBA, we measured the binding affinity, K_a, of free APBA for DHCA

317 by ^{1}H NMR spectroscopy titration. The measurements were performed at pH 6, i.e.
318 close to the pH of skin, and at pH 7.4, which is the pH of the hydrogel formulations.

319 The ^{1}H NMR spectra of APBA alone and in the presence of excess DHCA were
320 first recorded to easily assign the aromatic proton signals corresponding to bound and
321 unbound APBA (Fig. 2). Then, several ^{1}H NMR spectra of APBA/DHCA mixtures in
322 which the molar ratio of APBA/DHCA was varied from 1 to 2 were recorded to calculate
323 K_a as detailed in supporting information (Fig. S1 and S2).

324 The K_a value between DHCA and APBA was lower in acidic conditions (K_a =
325 130.5 ± 6.1 L/mol at pH 6) than at pH 7.4 (K_a = 1726.7 ± 28.4 L/mol). These data are
326 in line with the fact that the affinity between PBA and diol-containing molecules is pH
327 dependent (Yan, Springsteen, Deeter, & Wang, 2004). In particular, Springsteen and
328 Wang (Springsteen & Wang, 2002) found a K_a of 150 M^{-1} and 830 M^{-1} of the ester
329 formed between phenylboronic acid and catechol at pH 6.5 and pH 7.4, respectively.
330 These data suggest that the pH of skin may be used as a trigger for localized release
331 of DHCA complexed with APBA in the hydrogel formed at pH 7.4.
332

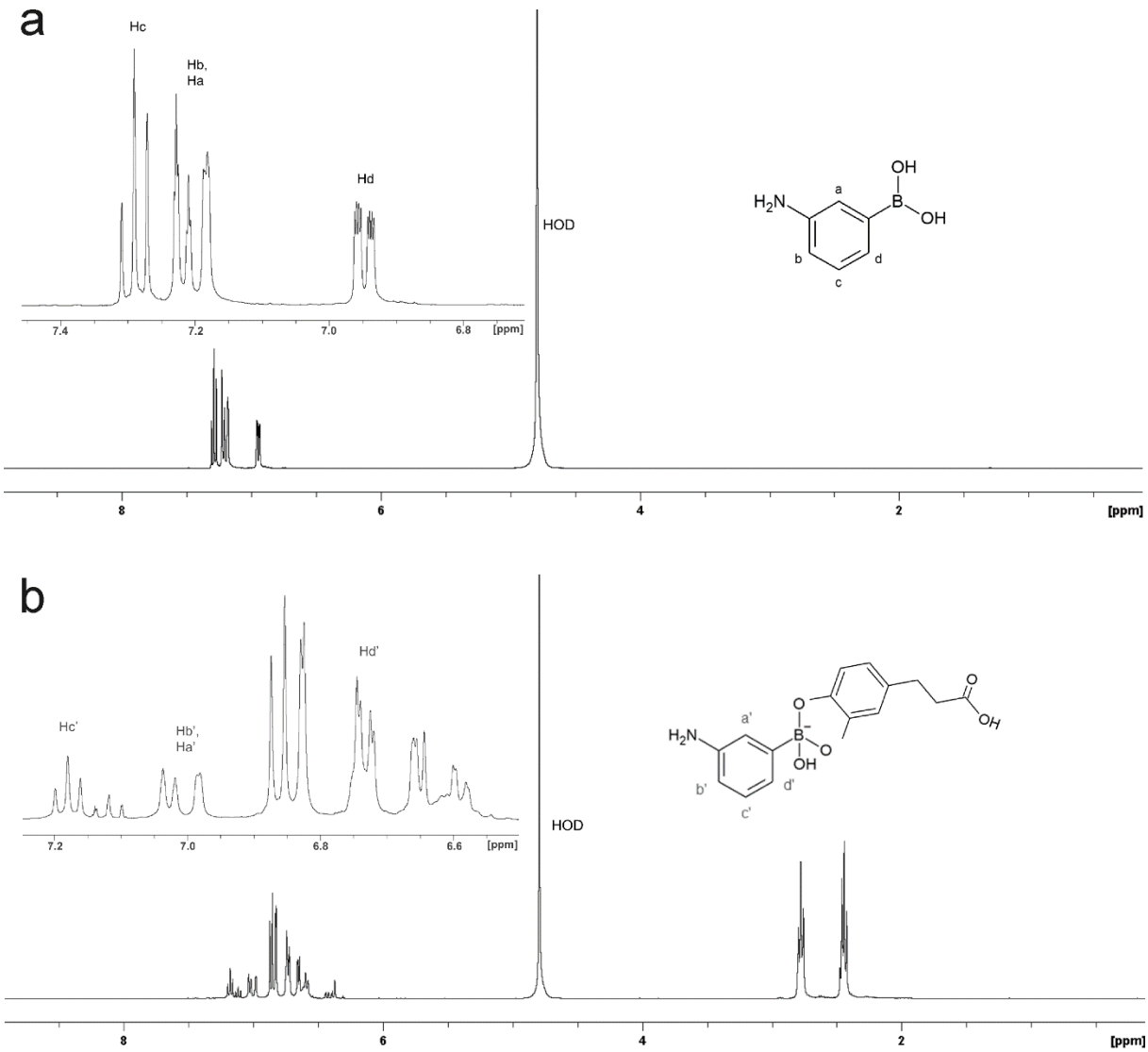

Figure 2: K_a determination between DHCA and APBA by ^{1}H NMR spectroscopy titration analysis. ^{1}H NMR spectra in 0.01 M deutered PBS pD 7.4 at 25 °C of APBA alone (18 mM) (a) and APBA (18 mM) in the presence of excess DHCA (54 mM) (b).

3.2. DHCA complexation by HA-PBA and formation of HG

In the present work, two HA derivatives modified with 3-aminophenyl boronic acid and with gluconamide moieties (HA-PBA and HA-GLU, respectively) were used to obtain a dynamic covalent hydrogel at physiological pH for complexation of DHCA. Indeed, we previously demonstrated formation of networks exhibiting a gel-like behavior at physiological pH by combining HA-PBA with HA-GLU. Such properties were related to the high binding capacity of PBA towards glucose units in the ring-opened form (such as gluconamide derivatives, resulting in the formation of boronate

346 ester bonds with slow exchange dynamics. By contrast, HA-PBA alone gives rise to a
347 viscous solution similar to initial HA, as PBA has nearly no affinity for HA sugars
348 (Figueiredo, Cosenza, et al., 2020).

349 The HA-PBA and HA-GLU derivatives were prepared by amide bond formation
350 between the carboxylic groups of HA and amine-fonctionalized GLU, using DMTMM
351 as a coupling agent (Figueiredo, Cosenza, et al., 2020). The structures of the HA-PBA
352 and HA-GLU conjugates were confirmed by ^{1}H and ^{13}C NMR spectroscopy,
353 respectively. Digital integration of the NMR spectra also allowed to assess their degree
354 of substitution (DS = 0.5 for HA-PBA and 0.1 for HA-GLU). Here, we targeted a DS
355 value for HA-PBA more than two-fold higher than HA-GLU so that half of the grafted
356 PBA is used for the selective complexation of DHCA.

357 Formation of the HA-PBA/DHCA complexes was carried out in 0.01 M PBS both
358 at pH 6 and pH 7.4. The values of DHCA complexation efficiency at pH 6 and pH 7.4
359 were found to be 50% and 58%, respectively. The difference between the two DCE
360 values is not so high given the K_a values found for the APBA/DHCA complex at these
361 two pH. However, the K_a values were measured for free APBA, which suggests some
362 positive impact of HA on the DHCA binding capability to PBA at pH 6.

363 Then, the HG at pH 6 and at pH 7.4 were obtained by simply mixing HA-
364 PBA/DHCA and HA-GLU, through boronate ester bond formation between the
365 remaining APBA moieties and the GLU molecules grafted on HA (Fig. S8). Plain HG
366 were also produced by mixing HA-PBA with HA-GLU in the same conditions (Fig. S9).

367 We confirmed hydrogels network formation by dynamic rheological
368 experiments. In our study, the frequency sweep measurements of the storage (elastic)
369 modulus (G') and the loss (viscous) modulus (G'') were performed to probe the gel-like
370 properties of the HA-PBA/HA-GLU network with and without DHCA under different pH

371 conditions. These measurements revealed a predominant elastic response for the HA-
372 PBA/HA-GLU assembly with and without DHCA at pH 7.4, as G' is higher than G"
373 within the whole range of frequencies covered (Fig. 3a). These data thus show that
374 these networks have a gel-like behavior. On the other hand, it was observed that for
375 both networks produced at pH 6, G'' dominates G' in a large range of frequency (Fig.
376 3b). Therefore, a viscous behavior predominates at pH 6. This decrease in the lifetime
377 of the network (G'-G" crossover point observed at higher frequency) and in the density
378 of cross-linking (decrease of the G' modulus) can be reasonably attributed to the
379 decrease of affinity of PBA for GLU at pH 6 (Tarus et al., 2014).

380 The difference in HG formation at pH 6 and at pH 7.4 is confirmed by the
381 analysis of G' at a fixed frequency of 2.5 Hz (Fig. 3c). G' values were lower for plain
382 HG and for HG containing DHCA produced at pH 6 (44.6 Pa and 28.1 Pa, respectively),
383 than G' values obtained for those produced at pH 7.4 (305.8 Pa and 296.1 Pa,
384 respectively). Moreover, it is worth noting that DHCA incorporation in the HG did not
385 hamper HG formation at both pHs, considering the similar rheological behavior for plain
386 HG and for HG containing DHCA (no statistically significant difference was found
387 between G' for HG produced at pH 6 and at pH 7.4, $p < 0.05$). Taking into account the
388 better DCE and the most adequate rheological properties of HG produced at pH 7.4,
389 they were chosen for further biological experiments.

390

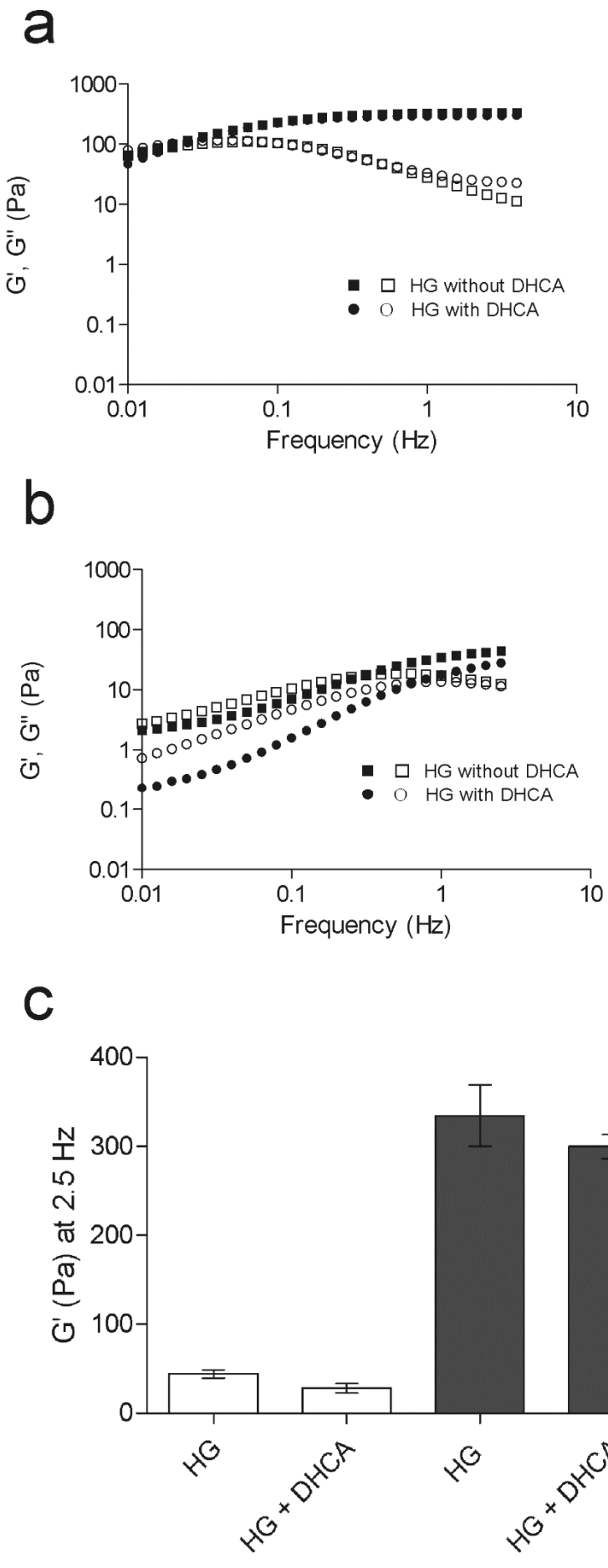
a
1000
100
10
1
0.1
0.01
G', G'' (Pa)
HG without DHCA
HG with DHCA
0.01
0.1
1
10
Frequency (Hz)
b
1000
100
10
1
0.1
0.01
G', G'' (Pa)
HG without DHCA
HG with DHCA
0.01
0.1
1
10
Frequency (Hz)
c
400
300
200
100
0
G' (Pa) at 2.5 Hz
HG
HG + DHCA
HG
HG + DHCA

391

Figure 3: Dependence of storage modulus (filled symbols) and viscous modulus (open symbols) on frequency of modified HA-hydrogels without DHCA and with DHCA at pH 7.4 (a) and pH 6 (b) at 32 °C, and storage modulus of modified HA-hydrogels without DHCA (HG) and with DHCA (HG + DHCA) at 2.5 Hz in pH 6 (white bars) and in pH 7.4 (gray bars) at 32 °C (c), and each column represents the mean ± SD (n = 3).

3.3. *In vitro* DHCA release studies

Delivery systems for topical administration that provide a controlled drug release are highly desired, given their potential benefits to the patient. Sustained release can prevent adverse effects caused by active ingredients present in high concentrations, supplies the skin for long periods, thereby reducing the number of product administrations, and decreases drug exposure to external environment. Therefore, such topical systems promote more safety and comfort for users, in addition to improve effectiveness of the drug (Costa & Santos, 2017).

The *in vitro* release of DHCA from HG was conducted using cell culture inserts positioned inside wells of a 24-well plate containing receptor media composed by 0.01 M PBS at pH 6 or pH 7.4. These two receptors medium were chosen to emphasize the different behavior of the HGs in a neutral environment and in a more acidic condition, similar to the skin environment. For comparison, cell culture inserts containing free DHCA dispersed in water were also prepared as blanks. Plates were kept under continuous stirring at 32 ºC (to reproduce the skin temperature) (Kregar et al., 2015) and the receiver solution was collected at pre-determined times for quantification of DHCA by HPLC. Fig. 4 compares plots of the cumulative release over time of DHCA solubilized in water (blank) and entrapped in the HG in receptor medium at pH 7.4 and pH 6. As expected, HG prolonged DHCA release in both receptor mediums, compared to the blank. In receptor medium at pH 7.4, only 9 % of DHCA was released from the HG while 36% release was achieved for the blank during 8 h. In receptor medium at

pH 6, 38% and 19% of DHCA release was measured for the blank and the HG formulation, respectively, in the 8 h of testing.

The fastest delivery of DHCA at pH 6 can be attributed to two main factors: the decreased number of boronate ester crosslinks in acidic conditions resulting in the formation of a loosely crosslinked HA network, and the reduced number of DHCA/PBA complexes. Both factors facilitate release of DHCA into the surrounding acidic environment compared to the physiological medium.

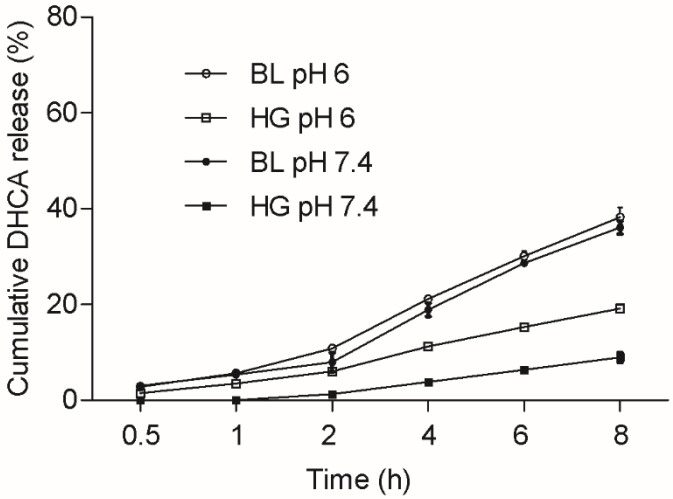

Figure 4: *In vitro* DHCA release from destiled water (blank-BL) and from modified HA-hydrogel (HG) produced at pH 7.4 in 0.01 M PBS pH 6.0 and pH 7.4 at 32 °C. Each symbol represents the mean ± SD (n = 3).

3.4. Cytotoxicity and protective effect of HG against UVB-induced cell death

Human skin confers physical, chemical, and bacteriological protection for the organism. Besides, skin prevents dehydration, participates to thermoregulation, hormone production, contains elements of immune system and expresses external beauty (Rittie & Fisher, 2015). Hence, the maintenance of a healthy skin presents a physiologic and social importance. Dermis plays important functions in skin: confers

structural and mechanical properties, and offers supplementation of nutrients for the epidermis (Duque, Bravo, & Osorio, 2017). Fibroblasts are the main cell type of the dermis, and they produce elastin and collagen fibers, proteoglycans and glycosaminoglycans, such as HA, which promotes hydration, skin stiffness, resistance to deformation, skin repair and wound healing (Britto et al., 2017; Duque et al., 2017; Haydont, Bernard, & Fortunel, 2018). For these reasons, several studies have been evaluated the detrimental effects of external insults in fibroblasts, including from UV radiation (Britto et al., 2017; Oliveira et al., 2019).

Oxidative stress promoted by UVB causes a set of keratinocytes and fibroblasts damages, which can result in skin disorders, such as photoaging and skin cancer (Dunaway et al., 2018). In our previous work, we demonstrated that DHCA is a promising antiaging agent, which could prevent UVB-induced oxidative stress and its damages to L929 cells (Oliveira et al., 2019).

In order to evaluate the effect of DHCA incorporation in the HG and its ability to counteract fibroblasts harms promoted by UVB, we firstly verified toxicity and then cytoprotection against UVB-induced L929 cell death of DHCA, plain HG and HG containing DHCA. The samples were not toxic to L929 cells in all range of concentrations evaluated (7 – 35 µM equivalent in DHCA), with a cell viability of 98%, 97% and 94% for the highest dose of DHCA (35 µM), plain HG (23 mg of HG) and HG containing DHCA (35 µM of DHCA in 23 mg of HG), respectively (Fig. 5).

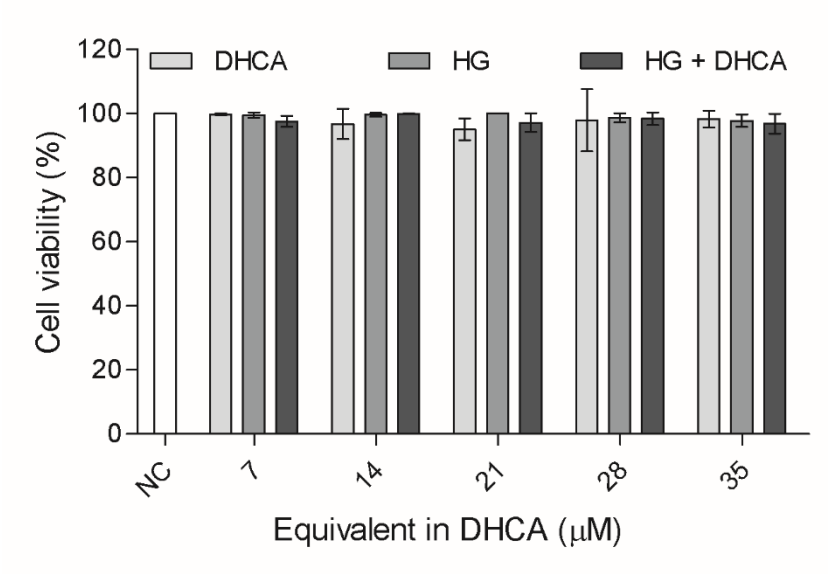

Figure 5: Effect of DHCA, plain modified HA-hydrogel (HG) and HG containing DHCA (7 – 35 μM of DHCA or hydrogels doses containing 7 – 35 μM of DHCA) in cell viability of L929 cells evaluated by neutral red assay after 24 h of treatment. Each column represents the mean ± SD (n = 3).

As shown by figure 6a, UVB irradiation significantly decreased cell viability at 600 mJ/cm^2 (cell viability of 52%) compared to nontreated and nonirradiated cells (NC), while 1 mM of *N*-acetyl cysteine, the standard antioxidant used, protected UVB-induced cell death (cell viability of 69%). As expected, DHCA alone showed a cytoprotective effect in a dose dependent manner (significant difference was observed between 7 μM and 35 μM of DHCA [$p < 0.01$], as well as between 14 μM and 35 μM of DHCA [$p < 0.05$]). A significant increase in the cell viability was obtained only at higher dose evaluated (cell viability of 65% at 35 μM of DHCA) (Oliveira et al., 2019). Interestingly, plain HG also protected L929 cells against death induced by UVB (cell viability of 68% for 23 mg of HG), and the HG containing DHCA provided a significant protective effect in all doses used (cell viability of 76% at 35 μM of DHCA in 23 mg of HG).

Microscopic analyses (Fig. 6b) confirmed the results described above. UVB induced a decrease in cell number and changes in cellular morphology. On the other

480 hand, 1 mM NAC and the samples evaluated partially restored cell number, and
481 improved cellular morphology, especially the HG containing DHCA.

482 These results are in agreement with our previous cytoprotective results for
483 DHCA alone. This phenolic compound prevented cell death by diminishing oxidative
484 stress and its cellular damages caused by UVB exposure (Oliveira et al., 2019).
485 Moreover, we observed a significative protection of plain HG, and that the incorporation
486 of DHCA in the HG improved the protection against death promoted by UVB, especially
487 in lower concentrations evaluated. HA, the main component of the HG, have shown
488 proliferative properties in human dermal fibroblasts by increases expression of
489 transforming growth factor-β (TGF-β), besides to promote collagen preservation
490 through induction of tissue inhibitor of metalloproteinase 1 (TIMP-1) expression, and
491 reduction of MMP-1 expression (Monteiro, Tersario, Lucena, Moura, & Steiner, 2013).
492 Taken together, these HA properties can contribute to the cytoprotective capacity
493 verified for HG. In addition, the higher cytoprotective capacity of the HG containing
494 DHCA can also be explained by the beneficial effects of HA on skin cells, which
495 improves the cytoprotection promoted by DHCA.
496

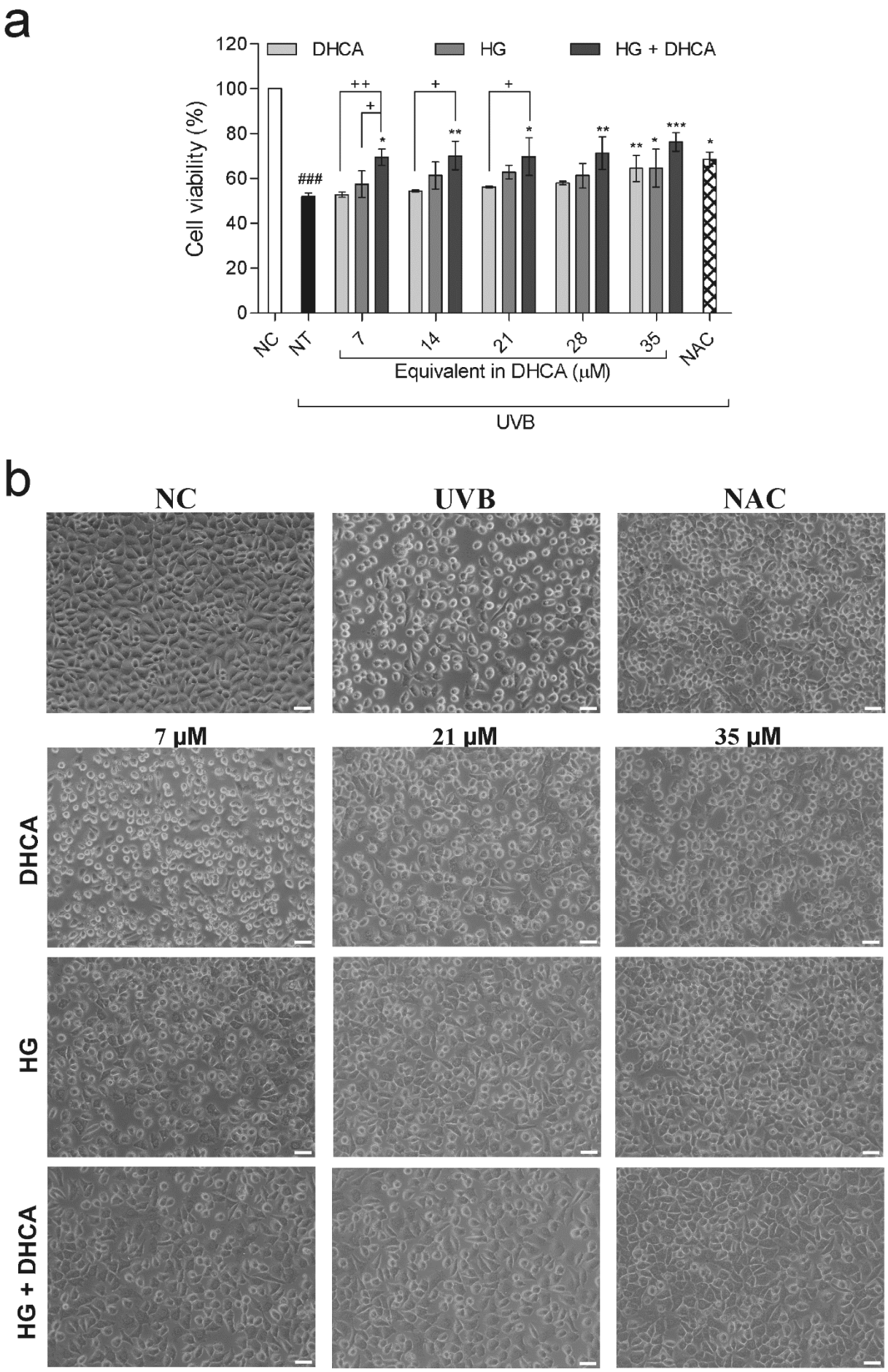
a
DHCA
HG
HG + DHCA
Cell viability (%)
120
100
80
60
40
20
0
NC
NT
7
14
21
28
35
NAC
Equivalent in DHCA (μM)
UVB
b
NC
UVB
NAC
7 μM
21 μM
35 μM
DHCA
HG
HG + DHCA

497

Figure 6: Cytoprotective effect of DHCA, plain dynamic covalent HA hydrogel (HG), HG containing DHCA (HG + DHCA) (7 - 35 µM of DHCA or hydrogels doses containing 7 - 35 µM of DHCA) and NAC (1 mM) against L929 cell death induced by UVB. L929 cells were pretreated for 1 h before UVB irradiation (600 mJ/cm^2), and after 24 h of irradiation cells were submitted to neutral red assay (a) or observed using a phase contrast inverted microscope (b). Each column represents the mean ± SD (n = 3). ### $p < 0.001$: significantly different from nonirradiated and nontreated cells (NC); * $p < 0.05$, ** $p < 0.01$ and *** $p < 0.001$: significantly different from irradiated and nontreated cells (NT); + $p < 0.05$, ++ $p < 0.01$. Scale bars: 50 μm.

4. Conclusions

In this work, a novel dynamic covalent HA hydrogel containing the antioxidant and anti-photoaging agent DHCA for skin applications was developed. We demonstrated the selective entrapment of DHCA in the hydrogel through its complexation with PBA grafted on HA chains via boronate ester bond formation. The system developed prolonged DHCA release using the pH as a trigger, which allows an effective release of DHCA in skin environment. Moreover, the skin beneficial properties of HA used to produce the hydrogel contributed to improve DHCA protection against UVB-induced fibroblasts death. In this way, the polysaccharide employed in the present study provided a set of advantages, considering that it participated in the dynamic covalent hydrogel production and in the mechanism to control DHCA release, as well as played an important role in fibroblasts protection against UVB. Therefore, the potential of a novel smart HA hydrogel produced in preventing skin photoaging for long periods make it a good candidate for future cosmetic applications.

Acknowledgements

The authors gratefully acknowledge CAPES/COFECUB program (Ph-C 911/18) for financial support and for scholarship provided to M. M. O. The authors also thank the NMR platform of ICMG (FR2607) for its support, and S. Ortega and T. Vilas Boas Figueiredo for technical and theoretical support, respectively.

Appendix A. Supplementary material

References

Amić, A., Marković, Z., Klein, E., Dimitrić Marković, J. M., & Milenković, D. (2018). Theoretical study of the thermodynamics of the mechanisms underlying antiradical activity of cinnamic acid derivatives. *Food Chemistry*, *246*, 481–489.

Avadhani, K. S., Manikkath, J., Tiwari, M., Godavarthi, A., Vidya, S. M., Hariharapura, R. C., et al. (2017). Skin delivery of epigallocatechin-3-gallate (EGCG) and hyaluronic acid loaded nano-transfersomes for antioxidant and anti-aging effects in UV radiation induced skin damage loaded nano-transfersomes for antioxidant and anti-aging effects. *Drug Delivery*, *24*(1), 61–74.

Bagde, A., Mondal, A., & Singh, M. (2018). Drug delivery strategies for chemoprevention of UVB-induced skin cancer : A review. *Photodermatology, Photoimmunology and Photomedicine*, *34*, 60–68.

Bérubé, M., Dowlut, M., & Hall, D. G. (2008). Benzoboroxoles as Efficient Glycopyranoside-Binding Agents in Physiological Conditions : Structure and Selectivity of Complex Formation Marie Be. *Journal Organic Chemistry*, *73*, 6471–6479.

Borenfreund, E., & Puerner, J. A. (1985). Toxicity determined in vitro by morphological alterations and neutral red absorption. *Toxicology Letters*, *24*, 119–124.

Britto, S. M., Shanthakumari, D., Agilan, B., Radhiga, T., & Kanimozhi, G. (2017). Apigenin prevents ultraviolet-B radiation induced cyclobutane pyrimidine dimers formation in human dermal fi broblasts. *Mutation Research - Genetic Toxicology*

553 *and Environmental Mutagenesis*, *821*, 28–35.
554 Brooks, W. L. A., & Sumerlin, B. S. (2016). Synthesis and Applications of Boronic
555 Acid-Containing Polymers : From Materials to Medicine. *Chemical Reviews*, *116*,
556 1375–1397.
557 Cavinato, M., & Jansen-Dürr, P. (2017). Molecular mechanisms of UVB-induced
558 senescence of dermal fi broblasts and its relevance for photoaging of the human
559 skin. *Experimental Gerontology*, *94*, 78–82.
560 Cavinato, M., Waltenberger, B., Baraldo, G., Grade, C. V. C., & Jansen-Durr, H. S. P.
561 (2017). Plant extracts and natural compounds used against UVB-induced
562 photoaging. *Biogerontology*, *18*, 499–516.
563 Costa, R., & Santos, L. (2017). Delivery systems for cosmetics - From manufacturing
564 to the skin of natural antioxidants. *Powder Technology*, *322*, 402–416.
565 Duffy, E., Guzman, K. De, Wallace, R., Murphy, R., & Morrin, A. (2017). Non-Invasive
566 Assessment of Skin Barrier Properties : Investigating Emerging Tools for In Vitro
567 and In Vivo Applications. *Cosmetics*, *4*(44), 1–14.
568 Dunaway, S., Odin, R., Zhou, L., Ji, L., & Zhang, Y. (2018). Natural Antioxidants :
569 Multiple Mechanisms to Protect Skin From Solar Radiation. *Frontiers in*
570 *Pharmacology*, *9*, 1–14.
571 Duque, L., Bravo, K., & Osorio, E. (2017). A holistic anti-aging approach applied in
572 selected cultivated medicinal plants: A view of photoprotection of the skin by
573 different mechanisms. *Industrial Crops and Products*, *97*, 431–439.
574 Essendoubi, M., Gobinet, C., Reynaud, R., Angiboust, J. F., Manfait, M., & Piot, O.
575 (2016). Human skin penetration of hyaluronic acid of different molecular weights
576 as probed by Raman spectroscopy. *Skin Research and Technology*, *22*, 55–62.
577 Este, M. D., Eglin, D., & Alini, M. (2014). A systematic analysis of DMTMM vs EDC /

578 NHS for ligation of amines to Hyaluronan in water. *Carbohydrate Polymers*, *108*,
579 239–246.
580 Figueiredo, T., Cosenza, V., Ogawa, Y., Jeacomine, I., Vallet, A., Ortega, S., et al.
581 (2020). Boronic acid and diol-containing polymers: how to choose the correct
582 couple to form “strong” hydrogels at physiological pH. *Soft Matter*, *16*, 3628–
583 3641.
584 Figueiredo, T., Jing, J., Jeacomine, I., Olsson, J., Gerfaud, T., Boiteau, J., et al.
585 (2019). Injectable Self-Healing Hydrogels Based on Boronate Ester Formation
586 between Hyaluronic Acid Partners Modi fi ed with Benzoxaborin Derivatives and
587 Saccharides. *Biomacromolecules*, *21*(1), 230–239.
588 Figueiredo, T., Ogawa, Y., Jing, J., Cosenza, V., Jeacomine, I., Olsson, J. D. M., et
589 al. (2020). Self-crosslinking smart hydrogels through direct complexation be-
590 tween benzoxaborole derivatives and diols from hyaluronic acid. *Polymer*
591 *Chemistry*, *11*, 3800–3811.
592 Haydont, V., Bernard, B. A., & Fortunel, N. O. (2018). Age-related evolutions of the
593 dermis: Clinical signs, fibroblast and extracellular matrix dynamics. *Mechanisms*
594 *of Ageing and Development*, *177*, 150–156.
595 Heleg-Shabtai, V., Aizen, R., Orbach, R., Aleman-Garcia, M. A., & Willner, I. (2015).
596 Gossypol-Cross Linked Boronic Acid-Modified Hydrogels: Functional Matrix for
597 the Controlled Release of an Anticancer Drug. *Langmuir*, *31*, 2237–2242.
598 Huang, Z., Delparastan, P., Burch, P., Cao, Y., Messersmith, P. B., & Cheng, J.
599 (2018). Injectable dynamic covalent hydrogels of boronic acid polymers cross-
600 linked by bioactive plant-derived polyphenols. *Biomaterials Science*, *6*, 2487–
601 2495.
602 ICH. (2005). International Conference on Harmonisation of Technical Requirements

603 for Registration of Pharmaceiticals for Human Use, Validation of Analytical
604 Procedures: Text and Methodology Q2(R1).
605 Kostova, B., Georgieva, D., Dundarova, M., Ivanova, S., Ivanova-mileva, K.,
606 Tzankova, V., & Christova, D. (2018). Design and study of the potential of
607 crosslinked cationic polymers as drug delivery systems for dermal application.
608 *Journal of Applied Polymer*, *46420*, 1–10.
609 Kregar, M. L., Dürrigl, M., Rozman, A., Jelcic, Ž., Cetina-cizmek, B., & Filipovic-Grcic,
610 J. (2015). Development and validation of an in vitro release method for topical
611 particulate delivery systems c. *International Journal of Pharmaceutics*, *485*, 202–
612 214.
613 Liang, Y., Zhao, X., Hu, T., Chen, B., Yin, Z., Ma, P. X., et al. (2019). Adhesive
614 Hemostatic Conducting Injectable Composite Hydrogels with Sustained Drug
615 Release and Photothermal Antibacterial Activity to Promote Full-Thickness Skin
616 Regeneration During Wound Healing. *Small*, *15*(12), 1–17.
617 Lou, J., Liu, F., Lindsay, C. D., Chaudhuri, O., Heilshorn, S. C., & Xia, Y. (2018).
618 Dynamic Hyaluronan Hydrogels with Temporally Modulated High Injectability
619 and Stability Using a Biocompatible Catalyst. *Advanced Materials*, *1705215*, 1–
620 6.
621 Marco-Dufort, B., & Tibbitt, M. W. (2019). Design of moldable hydrogels for
622 biomedical applications using dynamic covalent boronic esters. *Materials Today*
623 *Chemistry*, *12*, 16–33.
624 Mayumi, K., Marcellan, A., Ducouret, G., Creton, C., & Narita, T. (2013). Stress –
625 Strain Relationship of Highly Stretchable Dual Cross-Link Gels: Separability of
626 Strain and Time Effect. *ACS Macro Letters*, *2*, 1065–1068.
627 Monteiro, M. R., Tersario, I. L. dos S., Lucena, S. V., Moura, G. E. D. de D., &

628 Steiner, D. (2013). Culture of human dermal fibroblasts in the presence of
629 hyaluronic acid and polyethylene glycol: effects on cell proliferation, collagen
630 production, and related enzymes linked to the remodeling of the extracellular
631 matrix. *Surgical & Cosmetic Dermatology*, *5*(3), 222–225.
632 Nie, J., Pei, B., Wang, Z., & Hu, Q. (2018). Construction of ordered structure in
633 polysaccharide hydrogel: A review. *Carbohydrate Polymers*, *205*, 225–235.
634 Nimmo, C. M., Owen, S. C., & Shoichet, M. S. (2011). Diels - Alder Click Cross-
635 Linked Hyaluronic Acid Hydrogels for Tissue Engineering. *Biomacromolecules*,
636 *12*, 824–830.
637 Oliveira, M. M., Ratti, B. A., Daré, R. G., Silva, S. O., Truiti, C. T., Ueda-nakamura,
638 T., et al. (2019). Dihydrocaffeic Acid Prevents UVB-Induced Oxidative Stress
639 Leading to the Inhibition of Apoptosis and MMP-1 Expression via p38 Signaling
640 Pathway. *Oxidative Medicine and Cellular Longevity*, *2019*, 1–15.
641 Poquet, L., Clifford, M. N., & Williamson, G. (2008). Effect of dihydrocaffeic acid on
642 UV irradiation of human keratinocyte HaCaT cells. *Archives of Biochemistry and*
643 *Biophysics*, *476*(2), 196–204.
644 Rittie, L., & Fisher, G. J. (2015). Natural and Sun-Induced Aging of Human Skin. *Cold*
645 *Spring Harbor Perspectives in Medicine*, 1–15.
646 Roberts, B. M. C., Hanson, M. C., Massey, A. P., Karren, E. A., & Kiser, P. F. (2007).
647 Dynamically Restructuring Hydrogel Networks Formed with Reversible Covalent
648 Crosslinks. *Advanced Materials*, *19*, 2503–2507.
649 Sacco, P., Furlani, F., Paoletti, S., & Donati, I. (2019). pH-Assisted Gelation of
650 Lactose-Modi fi ed Chitosan. *Biomacromolecules*, *20*, 3070–3075.
651 Sahiner, N., Sagbas, S., Sahiner, M., Silan, C., Aktas, N., & Turk, M. (2015).
652 Biocompatible and biodegradable poly(Tannic Acid) hydrogel with antimicrobial

653 and antioxidant properties. *International Journal of Biological Macromolecules*,
654 *82*, 150–159.
655 Springsteen, G., & Wang, B. (2002). A detailed examination of boronic acid ± diol
656 complexation. *Tetrahedron*, *58*, 5291–5300.
657 Tarus, D., Hachet, E., Messager, L., Catargi, B., Ravaine, V., & Auzély-velty, R.
658 (2014). Readily Prepared Dynamic Hydrogels by Combining Phenyl Boronic
659 Acid- and Maltose- Modifi ed Anionic Polysaccharides at Neutral pH.
660 *Macromolecular Rapid Communications*, *35*, 2089–2095.
661 Trombino, S., Cassano, R., Bloise, E., Muzzalupo, R., Tavano, L., & Picci, N. (2009).
662 Synthesis and antioxidant activity evaluation of a novel cellulose hydrogel
663 containing trans -ferulic acid. *Carbohydrate Polymers*, *75*, 184–188.
664 Xu, J., Yang, D., Li, W., Gao, Y., Chen, H., & Li, H. (2011). Phenylboronate-diol
665 crosslinked polymer gels with reversible sol-gel transition. *Polymer*, *52*, 4268–
666 4276.
667 Yan, J., Springsteen, G., Deeter, S., & Wang, B. (2004). The relationship among pKa
668 , pH , and binding constants in the interactions between boronic acids and diols
669 — it is not as simple as it appears. *Tetrahedron*, *60*, 11205–11209.